Digital in-line holography with a single high-order harmonic pulse

Jörg Schwenke*[a], Xinkui He, Alexander Mai, Miguel Miranda, Anne L'Huillier

Department of Physics, Lund University, Lund, Sweden
*also at MAX-lab, Lund University, Lund, Sweden

ABSTRACT

In this paper, we review the optimization and characterization of a high-order harmonic generation (HHG) source for application in coherence imaging, and the use of this light source in a digital in-line holography setup. The high-order harmonic beam is generated by focusing a powerful infrared beam into an Ar gas cell. The length of the cell and the focusing parameters are optimized to maximize the HHG output. By spectrally filtering and focusing the generated harmonic beam and positioning a 2D detector, we obtain a table-top light source suitable for in-line holography, capable of recording a hologram with a single 40 fs XUV pulse. The reconstructed images have a spatial resolution in the micrometer range.

Keywords: digital holography, high-order harmonic generation, time-resolved imaging, single-shot, XUV

1. INTRODUCTION

X-ray microscopy has become a very important application at synchrotron facilities, where the high photon energy allows for imaging of non-periodic structures with nanometer spatial resolution. The radiation from an undulator can be spectrally filtered to yield a sufficiently monochromatic and coherent beam, while still maintaining enough flux to perform diffractive imaging or Fourier transform holography[1-4]. Recently, the advent of the free electron laser (FEL) has lead to a further improvement of the photon energy, flux, and coherence properties. Furthermore, the short pulse lengths achievable with a FEL source, being on the order of a few tens of femtoseconds, allow for imaging with a high time resolution, as recently demonstrated[5,6]. Laser based soft x-ray radiation produced by high-order harmonic generation is an interesting table-top source with even higher time resolution, down to a few hundred attoseconds. The generated light is spatially and temporally coherent and has a relatively narrow bandwidth[7,8]. High-order harmonic generation has been applied to imaging by several groups[9-11]. In our setup, a high-order harmonic pulse[12] is used to perform digital in-line holography[13,14]. The number of photons in a single pulse is sufficient to produce a high quality hologram. In the next section, we will recapitulate the harmonic generation process and discuss the beam properties, section 3 gives details on the holography setup. Section 4 gives a brief overview of the algorithm, and section 5 shows the experimental results.

2. LASER SYSTEM AND HARMONIC GENERATION

In high-harmonic generation, a high intensity laser is focused into a gas medium, which results in the emission of a harmonic spectrum. The process is usually explained in terms of the semi-classical three step model. The effect of the driving laser on the gas atoms is such that the Coulomb potential of the atoms is distorted, so that an electron can tunnel through the potential barrier into the continuum. This requires the laser field intensity to be sufficiently high, so that the potential barrier is deformed but the total ionization remains small. In the case of Ar gas, the laser intensity should be about 10^{14} W/cm^2. An electron that tunnels into the continuum is accelerated in the laser field until the field changes sign, upon which the electron turns around and is accelerated towards the atom again. There is a certain possibility for recombination with the atom, in which case a high-energy photon is emitted. The photon energy can be calculated using a classical model, where it is the sum of the binding potential energy I_p and kinetic energy W_{kin} of the returning electron, $W = W_{kin} + I_{p.}$. The maximum kinetic energy, is $W_{kin,max} = 3.2\ U_p$, where U_p is the time averaged kinetic energy of an electron oscillating in the laser field, $U_p = (e^2 I)/(2\ m_e\ c\ \varepsilon_0\ \omega^2)$. Here I is the laser intensity, and ω the fundamental laser

[a] E-Mail: jorg.schwenke@maxlab.lu.se

Holography: Advances and Modern Trends, edited by Miroslav Miler, Miroslav Hrabovský,
Proc. of SPIE Vol. 7358, 73580B · © 2009 SPIE · CCC code: 0277-786X/09/$18 · doi: 10.1117/12.834246

frequency. The process can occur every half-cycle of the driving laser, which results in a spectrum that only consists of odd harmonics of the driving field frequency, up to the so-called cut-off energy of $W_{CO} = 3.2\ U_p + I_p$.

The laser system used to generate the harmonics is the low-power arm of the 40 TW laser at the High Power Laser Facility in Lund. It is a Ti:sapphire chirped pulse amplification laser and delivers 800 nm pulses at a 10 Hz repetition rate, 40 fs duration, and about 150 mJ energy before compression. The infrared pulses are delivered to the HHG beamline, which is shown in figure (1). A focusing lens with a focal length of 2 m focuses the infrared field. The beam can be apertured by an iris to adjust the intensity and beam diameter. Typically, only about 10 mJ are actually focused into the gas cell. The gas cell consists of a stack of thin metal plates, which have a cylindrical hole at the centre. By varying the number of plates, the length of the cylindrical volume can be adjusted. The gas is introduced from the central plate, which is mounted to the gas discharge setup. A piezo driven valve, triggered by the laser system, feeds gas through a thin tube into the central plate, from where it disperses along the cylindrical volume.

Figure (2a) shows a typical spectrum of the generated harmonic beam, and table (1) gives values for the pulse energies, photon numbers, and conversion efficiencies for the different harmonics, calculated from experimental data. For the holography experiment, the 21st harmonic was used. The gas cell length was 15 mm, the infrared energy focused into the cell was around 6 mJ. The photon number in a single pulse is in the order of $3\text{x}10^{10}$ per harmonic, which gives energies of about 160 nJ per harmonic[12]. For the 21st harmonic, $\Delta\lambda/\lambda$ is about 2×10^{-2}.

Figure (2b) shows the spatial profile of the harmonic beam. The pulse consists of a weak, divergent part, and a central part which is less divergent and has a higher intensity. The intense central part of the 21st harmonic, which is used for the imaging, has a half-angle of divergence of about 0.7 mrad.

3. IN-LINE HOLOGRAPHY SETUP

The generated harmonic beam is first filtered by a 200 nm thick Al filter to remove the remaining infrared light. The higher-order harmonics are strongly attenuated in the process, both by the Al filter and layers of oxygen. The transmission is between 13 and 21 % (table (1)). The beam is then focused by a Schwarzschild objective, which consists of a convex and a concave mirror whose centres of curvature coincide. The mirrors are multilayer coated to spectrally select the 21st harmonic (38 nm). To avoid specular back-reflection from the convex mirror, the objective is aligned off-axis, which causes the beam to exit the objective under an angle of about 8° towards the optical axis. The focus has a diameter of about 1 μm, at a position 5 cm behind the objective. This provides a divergent beam after the objective, with a half-angle of divergence of about 23 mrad. The focal spot is considered to be the point source for an in-line holography imaging scheme. A sample can be mounted on a three-axis motorized translation stage, which allows movement of the object over 13 mm in each direction, allowing for precise positioning in the divergent beam. The movement range along the beam axis includes the focal spot position. The distance between the detector and the focal spot is about 17 cm. The detector consists of a micro channel plate (MCP) and a CCD camera, which is triggered by the laser system.

4. ALGORITHM

The algorithm used to reconstruct the object from a recorded hologram is based on propagation of the electric field between the object plane and the hologram plane. It numerically solves the Fresnel-Kirchhoff integral by Fast Fourier Transformation[13]. Propagation can be carried out in both directions, meaning that a hologram can be simulated from an object function and an object can be reconstructed from an experimentally obtained hologram.

Besides the beam parameters, the algorithm also requires knowledge of the distances in the holography scheme. The distance between the object and the focal spot (point source position) can be found by moving the object across the focus, using a motorized translation stage with a position indicator. The distance to the detector, however, cannot be trivially measured. We solve the problem by reconstructing the object at several distances and identifying the correct object position in relation to the detector. This requires knowledge of the object shape, or calibration with a known object.

Due to the in-line geometry, the reconstructed real image overlaps with the virtual image (twin image). The presence of the out-of-focus virtual image adds blur to the image and reduces the image quality. In our algorithm, we use an iterative

phase retrieval algorithm suggested by Latychevskaia and Fink to reduce the blurring[15].

In this algorithm, the real intensity distribution recorded by the MCP is first combined with the phase of the reference wave. The complex field is then back-propagated to the object plane, and multiplied by the complex conjugated reference wave to yield the complex object function. The real amplitude of this function describes the absorption properties of the object. The algorithm checks the two dimensional function for negative absorption values (transmission larger than 1), which are attributed to the virtual image. By resetting the transmission to 1, the virtual image effect can be reduced.

This new function is recombined with the phase angle and forward propagated to the hologram plane. This is done to obtain the simulated phase of the object, which is then combined again with the recorded intensity distribution to form a new hologram. Running the loop sufficiently long should in principle result in the phase and amplitude properties of the object to develop towards their true value.

5. RESULTS

For these measurements, tungsten microscope tips were used as sample objects. The tips are produced by etching, and have an extremely narrow tip, which can be as small as a single atom[16]. Figure (3a) shows a hologram that was taken with a single pulse of the harmonic beam, after background subtraction, where the background was averaged over a large number of shots in the absence of the object. Figure (3b) shows the first reconstruction, and fig. (3c) shows the result of the iteration process. The first reconstruction shows blurring and additional fringes, the application of the iteration does improve the image quality, resulting in a better contrast and reduction of blurring.

Figure (4a) shows a hologram of the same tip, where the hologram was averaged over a large number of individual images. The subtracted background was averaged as well. It can be noted that the use of an averaged hologram (and background) results in a considerable reduction of noise in the recorded hologram. However, this does not result in a notably higher spatial resolution. The figures (4b) and (4c) show the reconstruction from this hologram without and with phase iteration, respectively. Again, the fringes and blurring seen in the first reconstruction are reduced by applying the phase iteration, but are still present.

To compare the single-shot and multiple-shot images, we consider the far edge of the tips in the reconstructed images, and determine the width of the tips (fig. (5)). The tip width is an upper estimate of the spatial resolution, and values of 4.7 and 4.3 μm for the multi-shot and single-shots holograms, respectively, were found. In this particular case, the single shot image has a better spatial resolution than the multiple-shot image. We note that the photon number in the harmonic beam is sufficient to produce single-shot holograms with roughly the same quality as the averaged shots. In other words, there is no gain in spatial resolution by averaging over a large number of shots.

The spatial resolution, however, is less than expected. A theoretical limit for the spatial resolution R is given by the divergence of the beam, according to $R = \lambda / (2 \sin(\phi))$, where ϕ is the half-angle of aperture after the focal point of the objective and $\sin(\phi)$ is the numerical aperture. The angle ϕ becomes maximal, if the size of the harmonic beam fills the available space in the off-axis position of the Schwarzschild convex mirror, without being clipped by the casing of the objective. The transmission of the beam through the objective has been simulated with the FRED raytracing software to estimate the maximal achievable beam divergence. By using a harmonic beam with a half-angle of divergence of 1.4 mrad, the half-angle divergence after the objective is about 34 mrad, when keeping the distance between the gas cell and the objective the same as in the present setup. In this case, the expected resolution is about 550 nm. From the experiment, however, the harmonic beam divergence is found to be about 0.7 mrad, and it cannot be increased without a significant reduction of the intensity. The focused harmonic beam has a half-angle divergence of $\phi = 23$ mrad, which suggests a resolution limit of $R = 820$ nm for the present setup.

There are several reasons why the theoretical spatial resolution is not achieved. An important factor is the recording of the hologram with the CCD camera. If the camera is unable to resolve the fine fringes of the hologram, the high spatial frequencies, which encode the sharp edges of the sample, cannot be reconstructed. This leads to blurred edges in the reconstructed image. In the present setup, a CCD camera is used, which does not meet the resolution of the MCP.

Another factor is the broad transmission curve of the objective, which is not limited to the 21st harmonic, but also allows significant transmission of at least one more harmonic, presumably the 23rd harmonic at 35 nm. This results in the forming of two holograms (or more) on the detector. By reconstructing the hologram with a single wavelength, the additional holograms are out of focus and add to the blur in the image.

During the experiments, it was also found that the XUV beam exhibits a significant instability in both pointing and intensity, which is a direct consequence of the instability of the driving laser. This does affect the measurements, since the background images and the multiple shot holograms are averaged over a large number of shots. The movement of the beam results in a distorted beam shape in the background images, which makes it difficult to subtract it cleanly from the acquired holograms. The backdrop surrounding the object can be seen to be not uniform, most pronounced in the multi-shot images (fig. (4)). Also, the line-out shown in figure (5) exhibits a superimposed variation of the transmission curve, due to the averaging over mismatching beam positions and intensities. This makes it difficult to identify and effectively remove the contributions of the virtual image, so that the iterative phase retrieval does not reach its full potential. The situation can be resolved by avoiding averaging of the images, and by improving the stability of the driving laser.

6. CONCLUSION

We have developed a coherent imaging beamline which consists of an optimized HHG source and an in-line holography setup. Holograms can be recorded with a single shot of the laser system, with pulse duration of 40 fs. The reconstructed images have a spatial resolution of about 4 μm. The spatial resolution is limited by the detector resolution, the transmission properties of the focusing optics, and the shot-to-shot instability of the laser system. An iterative phase retrieval algorithm is applied to reduce the appearance of the virtual image. We believe that the performance of the phase retrieval in particular is limited by the laser instability, and that recent improvements to laser stability and an upgrade of the detector will improve the spatial resolution towards the theoretical limit of the present setup, which is about 1 μm.

In the continuation of this project, the next steps are the imaging of phase objects, which depends strongly on the performance of the phase retrieval, and a pump-probe experiment, in order to demonstrate the temporal resolution of the technique.

ACKNOWLEDGMENTS

This research was supported by the Marie Curie Early Stage Training Site (MAXLAS), the Knut and Alice Wallenberg Foundation and the Swedish Research Council. We also thank Ulf Johansson and Ralf Nyholm for fruitful discussions and support.

REFERENCES

[1] Dierolf, M., Bunk, O., Kynde, S., Thibault, P., Johnson, I., Menzel, A., Jefimovs, K., David, C., Marti, O., Pfeiffer, F., “Ptychography & lensless X-ray imaging”, Europhys. News 39(1) 22-24 (2008)

[2] Miao, J., Hodgson, K. O., Ishikawa, T., Larabell, C. A., LeGros, M. A., Nishino, Y., “Imaging whole Escherichia coli bacteria by using single-particle x-ray diffraction”, Proc. Nat. Acad. Sci. U.S.A., 100(1), 110-112 (2003)

[3] Schlotter, W. F., Lüning, J., Rick, R., Chen, K., Scherz, A., Eisebitt, S., Günther, C. M., Eberhardt, W., Hellwig, O., Stöhr, J., “Extended field of view soft x-ray Fourier transform holography: toward imaging ultrafast evolution in a single shot”, J. Opt. Lett. 32(21), 3110–3112 (2007)

[4] Shapiro, D., Thibault, P., Beetz, T., Elser, V., Howells, M., Jacobsen, C., Kirz, J., Lima, E., Miao, H., Neiman, A. M., Sayre, D., “Biological imaging by soft x-ray diffraction microscopy”, Proc. Natl. Acad. Sci. U.S.A. 102(43), 15343–15346 (2005)

[5] Bogan, M. J., Benner, W. H., Boutet, S., Rohner, U., Frank, M., Barty, A., Seibert, M. M., Maia, F., Marchesini, S., Bajt, S., et al., “Single Particle X-ray Diffractive Imaging”, Nano Lett. 8(1), 310–316 (2008)

[6] Chapman, H. N., Hau-Riege, S. P., Bogan, M. J., Bajt, S., Barty, A., Boutet, S., Marchesini, S., Frank, M., Woods, B. W., Benner, W. H., et al., "Femtosecond time-delay X-ray holography", Nature 448, 676–680 (2007)

[7] Bartels, R. A., Paul, A., Green, H., Kapteyn, H. C., Murnane, M. M., Backus, S., Christov, I. P., Liu, Y., Attwood, D., Jacobsen, C., "Generation of Spatially Coherent Light at Extreme Ultraviolet Wavelengths", C. Science. 297, 376–378 (2002)

[8] Merdji, H., Salières, P., Le Déroff, L., Hergott, J.-F., Carré, B., Joyeux, D., Descamps, D., Norin, J., Lyngå, C., L'Huillier, A., Wahlström, C.-G., Bellini, M., Huller, S., "Coherence properties of high-order harmonics: Application to high-density laser–plasma diagnostic", Laser and Part. Beams 18, 495–502 (2000)

[9] Morlens, A.-S., Gautier, J., Rey, G., Zeitoun, P., Caumes, J.-P., Kos-Rosset, M., Merdji, H., Kazamias, S., Cassou, K., Fajardo, M.,"Submicrometer digital in-line holographic microscopy at 32 nm with high-order harmonics", M. Opt. Lett. 31(21), 3095–3097 (2006)

[10] Sandberg, R. L., Paul, A., Raymondson, D. A., Hädrich, S., Gaudiosi, D. M., Holtsnider, J., Tobey, R. I., Cohen, O., Murnane, M. M., Kapteyn, H. C., "Lensless Diffractive Imaging Using Tabletop Coherent High-Harmonic Soft-X-Ray Beams", Phys. Rev. Lett. 99, 098103-1–4 (2007)

[11] Tobey, R. I, Siemens, M. E., Cohen, O., Murnane, M. M., Kapteyn, H. C., Nelson, K. A, "Ultrafast extreme ultraviolet holography: dynamic monitoring of surface deformation", Opt. Lett. 32, 286–288 (2007)

[12] He, X., Miranda, M., Schwenke, J., Guilbaud, O, Ruchon, T., Heyl, C., Georgadiou, E., Rakowski, R., Persson, A., Gaarde, M. B. and L'Huillier, A., "Spatial and spectral properties of the high-order harmonic emission in argon for seeding applications", submitted to Phys. Rev. A in April 2009

[13] Genoud, G., Guilbaud, O., Mengotti, E., Pettersson, S.-G., Georgiadou, E., Pourtal, E., Wahlströhm, C.-G., and L'Huillier, A., "XUV digital in-line holography using high-order harmonics", Appl. Phys. B 90, 533-538 (2008)

[14] Schwenke, J., Mai, A., Miranda, M., He, X., Genoud, G., Mikkelsen, A., Pettersson, S.-G., Persson, A., and L'Huillier, A., "Single-shot holography using high-order harmonics", J. Mod. Opt. 55 (16), 2732, (2008)

[15] Latychevskaia, T., Fink, H.-W., "Solution to the Twin Image Problem in Holography", Phys. Rev. Lett. 98, 233901-1–4 (2007)

[16] Ekvall, I., Wahlström, E., Claesson, D., Olin, H., Olsson, E., "Preparation and characterization of electrochemically etched W tips for STM", Meas. Sci. Technol. 10, 11–18 (1999)

FIGURES

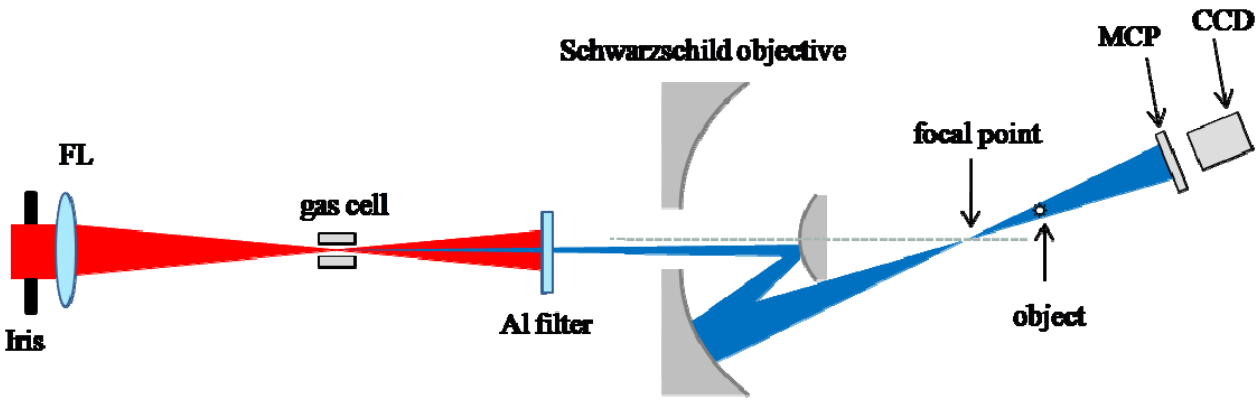

Figure 1: Experimental setup (not to scale). FL denotes the focusing lens with a focal length of 2 m.

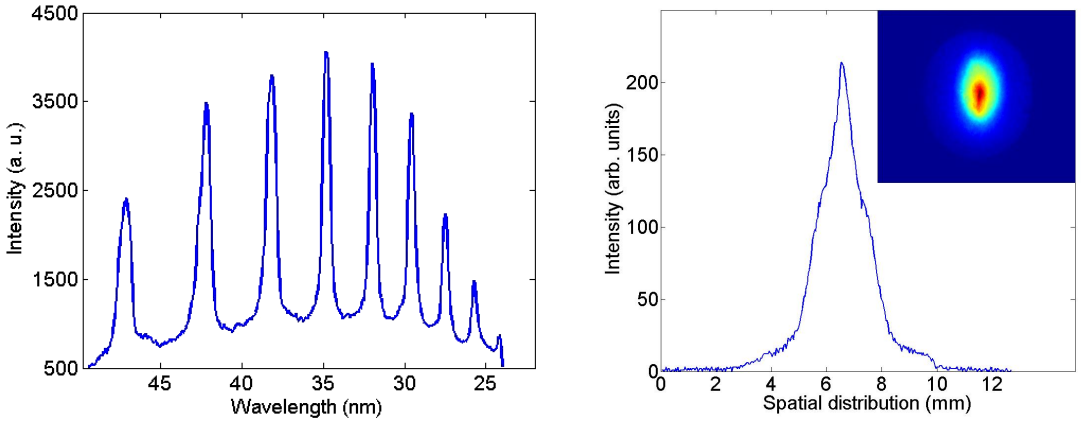

Figure 2: a) Spectrum of the harmonic pulse generated in the gas cell, b) spatial profile of the harmonic pulse, the inset shows the image of the beam on the detector[12].

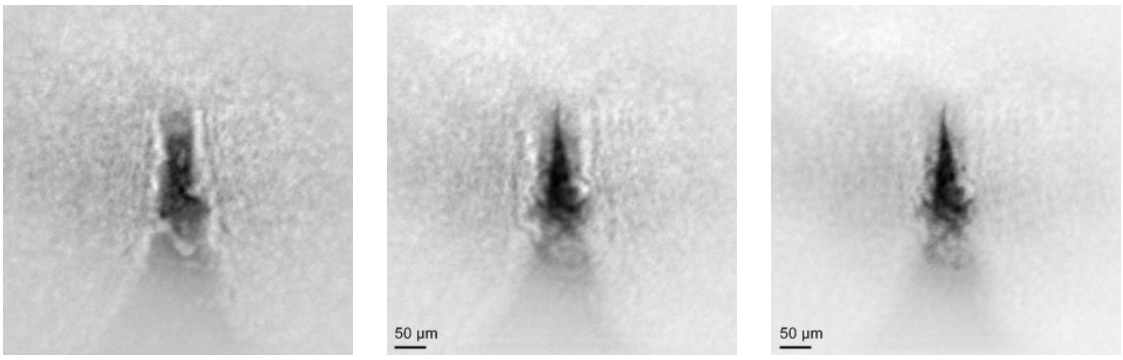

Figure 3: a) Single-shot hologram, b) reconstruction without phase retrieval iteration, c) reconstruction with phase retrieval[14].

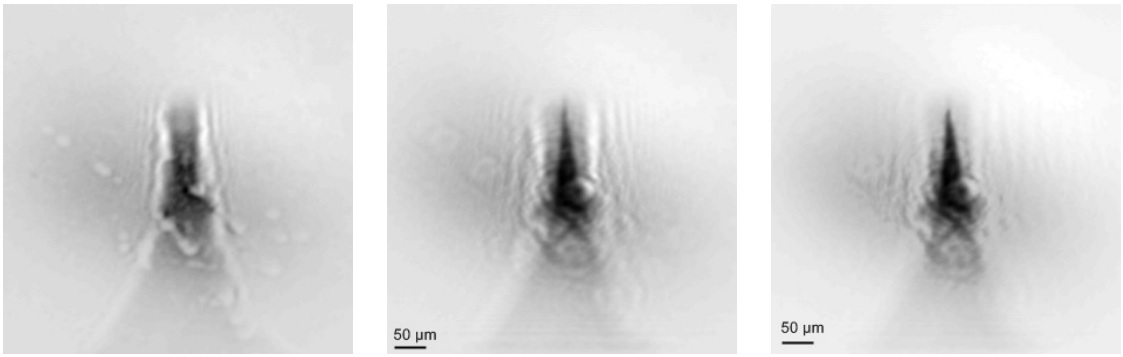

Figure 4: a) Multiple-shot hologram, b) reconstruction without phase retrieval iteration, c) reconstruction with phase retrieval[14].

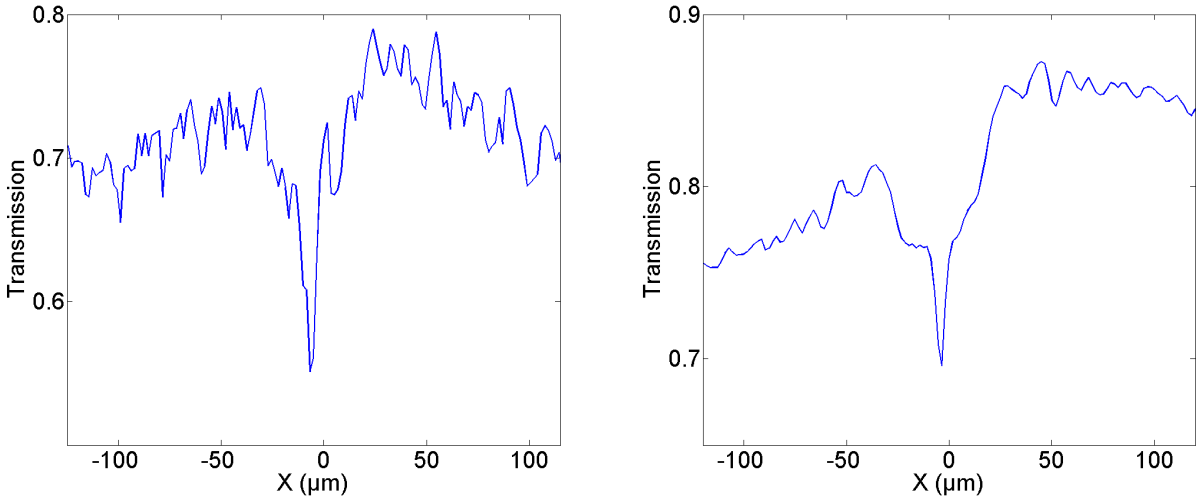

Figure 5: a) Line out at the end of the tip, showing tip width in a single-shot hologram reconstruction. b) Line out from the reconstruction of a multiple-shot hologram.

TABLES

Harmonic order	17	19	21	23	25	27
Transmission	0.12	0.13	0.15	0.16	0.19	0.21
Photon number ($\times 10^{10}$)	3.03	2.98	3.10	2.63	1.60	1.41
Energy (µJ)	0.13	0.14	0.16	0.15	0.10	0.09
Efficiency ($\times 10^{-6}$)	6.8	7.5	8.6	8.0	5.3	5.0

Table 1: Properties of the generated harmonics with optimized HHG setup[12].